9-1-2001

Collision-Induced Electronic Energy Transfer From v=0 Of The E(0g+) Ion-Pair State In I2: Collisions With I2(X)

Christopher J. Fecko , '98

Miriam Arak Freedman , '00

Thomas Alex Stephenson
Swarthmore College, tstephe1@swarthmore.edu

Recommended Citation

Collision-induced electronic energy transfer from v=0 of the E(0 g +) ion-pair state in I 2 : Collisions with I 2 (X)

Christopher J. Fecko, Miriam A. Freedman, and Thomas A. Stephenson

Collision-induced electronic energy transfer from $v=0$ of the $E(0_g^+)$ ion-pair state in I₂: Collisions with I₂(X)

Christopher J. Fecko,[a] Miriam A. Freedman,[b] and Thomas A. Stephenson[c]
Department of Chemistry, Swarthmore College, Swarthmore, Pennsylvania 19081

The collision-induced electronic energy transfer that occurs when I₂ in the $E(0_g^+)$ ion-pair electronic state collides with ground electronic state I₂ has been investigated. We prepare I₂ in single rotational levels in $v=0$ of the E state using two-color double resonance laser excitation. The resulting emission spectrum shows that the nearby ($\Delta T_e = -385 \text{ cm}^{-1}$) $D(0_u^+)$ electronic state is populated. The cross section for collision-induced $E \rightarrow D$ energy transfer is found to be $18 \pm 3 \text{ Å}^2$. A range of D state vibrational levels are populated, consistent with a model in which overlap between the initial and final vibrational wave functions is important, but modulated by propensities for small vibrational energy gaps and those energy gaps that are closely matched to the $v=0 \rightarrow v=1$ energy separation in the I₂(X) collision partner. © *2001 American Institute of Physics.*
[DOI: 10.1063/1.1391264]

I. INTRODUCTION

Interest in the inelastic collision dynamics of electronically excited I₂ dates to the early years of the 20th century, when Franck and Wood first examined the fluorescence from iodine in the presence of several foreign gases.[1] In the past 40 years, numerous detailed examinations of the rovibrational energy transfer processes that accompany collisions between buffer gases and I₂ in the ground $X(0_g^+)$ electronic state and the excited $B(0_u^+)$ electronic state have been carried out.[2–11] The level of detail gleaned from these studies is so large that the inelastic collision dynamics of I₂ have become benchmarks for the field of gas phase dynamics. In addition, quenching of I₂ in the B state by buffer gases has been the subject of extensive investigation, with collision-induced electronic predissociation being a principle means of depleting the excited state population.[2,12–16] This process occurs with both rare gas collision partners, as well as self-quenching [i.e., in collisions with I₂(X)].

In the work described in this paper we explore the inelastic electronic energy transfer processes that arise when I₂, prepared with $\approx 41\,000 \text{ cm}^{-1}$ of electronic energy, collides with I₂ in the ground electronic state. Specifically, we have examined the collision-induced electronic energy transfer processes that occur following excitation to single rotational levels in the lowest vibrational level of the $E(0_g^+)$ ion-pair electronic state. The E state is one of six strongly bound ($D_e \approx 31\,000 \text{ cm}^{-1}$), closely spaced electronic states, all correlating with the ionic atoms $I^+(^3P_2) + I^-(^1S_0)$. In order of increasing values of T_e, these states carry the historic labels (and Ω quantum numbers) $D'(2_g)$, $\beta(1_g)$, $D(0_u^+)$, $E(0_g^+)$, $\gamma(1_u)$, and $\delta(2_u)$. The T_e values range

from $40\,388 \text{ cm}^{-1}$, (D') (Ref. 17) to $41\,788 \text{ cm}^{-1}$ (δ).[18] The experiments described here are part of a larger, comprehensive investigation of the inelastic collision dynamics of I₂ in the ion-pair electronic states. In future publications we will describe the results of our studies of the electronic energy transfer and rotational/vibrational energy transfer that occurs when I₂(E) collides with a variety of rare gas species.

The electronic relaxation of I₂ in the E ion-pair state by collisions with I₂(X) was first reported by Ubachs *et al.*[19] (Evidence for a similar process in higher energy ion-pair states of I₂ was first noted, but not analyzed, by Heeman *et al.*[20]) In the former work, a single rotational level in $v=8$ in the E state was populated, and emission was observed from the nearby D electronic state ($\Delta T_e = -385 \text{ cm}^{-1}$) along with the dominant emission features characteristic of the E state. The relaxation process is found to populate several vibrational levels in the D state, though the distribution of rotational states is quite narrow.[19] In a more recent report from the same laboratory, Teule *et al.*[21] have extended the initial excitation to a range of E state vibrational levels.[20] In addition, Inard *et al.* have examined the collision-induced electronic energy transfer that occurs when I₂ is prepared in $v=1$ in the E electronic state.[22] Again, a number of different D state vibrational levels are populated.

A central unresolved issue that these investigations raise is the importance of vibrational energy gaps and vibrational wave function overlap in modulating the distribution of vibrational energy in the D electronic state. Energy gap and Franck–Condon models for vibrational populations in electronic energy transfer processes have been applied to a variety of systems, with widely varying degrees of success.[23] To date, there is no general consensus on which models are most applicable in which situations. This result arises dramatically in the case of the work by Teule *et al.*[21] These workers find that energy gap effects appear to dominate the dynamics for certain initial E state vibrational levels, while Franck–Condon effects are important for other vibrational levels.

Perhaps the most striking report of I₂$(E) + I₂(X)$ colli-

---
[a]Current address: Department of Chemistry, Massachusetts Institute of Technology, Cambridge, MA 02139.
[b]Current address: Department of Mathematics, University of Minnesota, Minneapolis, MN 55455.
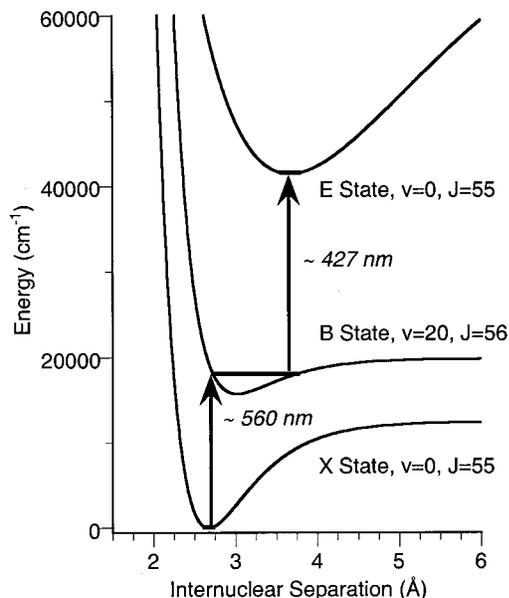[c]Author to whom all correspondence should be addressed. Electronic mail: tstephe1@swarthmore.edu

FIG. 1. Schematic of the double resonance excitation scheme used to populate $v=0$, $J=55$ in the E ion-pair state of I_2.

sion dynamics is the recent work by Akopyan *et al.*, in which I_2 is prepared in the E state in a range of higher vibrational levels ($v=23-58$).[24,25] In contrast to the results cited above, these investigators find that Franck–Condon effects have little to no importance in determining the D state vibrational populations. The D state level that is closest in energy to the initially excited E state level dominates the vibrational distribution by a factor of 10 or more. In addition, the overall cross section for electronic energy transfer is found to be huge, $>10^3 \text{ Å}^2$.[24,25] These results differ considerably from those reported here, and may point to an interesting qualitative variation of the electronic energy transfer process with E state vibrational excitation.

With the goal of shedding light on the substantial range of published results, in this paper we report on the population of the D electronic state that results from collisions of $I_2(E)$ in single rotational levels of the ground vibrational state. We consider two different initial rotational states ($J=55$ and 98) and extend the studies to I_2 pressures that are significantly lower than those used in any of the previous investigations, assuring that single collision conditions are securely met. While our goal of resolving the varying interpretations of the self-quenching of $I_2(E)$ has not been achieved, our results suggest that both Franck–Condon and energy gap effects are important, with the balance determined by the overall magnitude of the energy gaps involved.

II. EXPERIMENT

In these experiments, we prepare I_2 in single rotational levels of the lowest vibrational level of the E ion-pair electronic state using two-color double resonance excitation. Figure 1 is a schematic drawing of the excitation scheme used to prepare $J=55$. The initial $B \leftarrow X$ excitation occurs via the $(20,0)$, $R(56)$ transition; the required 559.95 nm radiation is provided by a Nd^{3+}–YAG pumped dye laser (Continuum Lasers YG580-30/TDL-50) operating with Rhodamine 590

laser dye (Exciton). After a delay of 5–10 nanoseconds, the second photon excites a fraction of the B state population using the $E \leftarrow B$ $(0,20)$, $P(56)$ transition at 426.56 nm. This photon is provided by a N_2-pumped dye laser (Laser Photonics UV24/DL-14P) operating with Coumarin 440 laser dye (Exciton). To prepare $J=98$ in the E state, the YAG-pumped and N_2-pumped dye lasers are tuned to the $B \leftarrow X$ $(21,0)$, $P(98)$ and the $E \leftarrow B$ $(0,21)$, $R(97)$ transitions at 559.96 nm and 428.66 nm, respectively. Both lasers have a pulse width of 10 nanoseconds. The timing between the excitation lasers is controlled by a digital delay generator (Princeton Applied Research 9650) and is variable over a wide range of delays. The emission features reported here occur only when the N_2 laser system fires coincident with or later than the YAG laser system; no emission is observed when one of the laser beams is blocked from reaching the sample chamber.

Double resonance excitation of I_2 results in intense $E \rightarrow B$ emission between 415 and 435 nm, as well as a number of weaker features, depending on the sample pressure conditions. I_2 emission is collected by an $f/1.2$ fused silica optical system, and is focused onto the entrance slit of a 0.5 m focal length scanning monochromator (Instruments SA 500 M). The monochromator is equipped with a 2400 groove/mm grating, providing a dispersion of 0.8 nm/mm. Typical slit widths were 200 microns. Wavelength resolved emission exiting the monochromator was detected by one of two methods. With the monochromator operating in scanning mode, emission was detected using a UV sensitive photomultiplier tube (Thorn/EMI 9613QB) mounted on the exit slit body. The output of the phototube was routed to a gated integrator (Stanford Research Systems SR250), with integrated emission intensities eventually stored on a laboratory computer using Labview software (National Instruments). Alternatively, the monochromator can operate as a spectrograph and a CCD camera (Princeton Instruments LN/CCD-2500PB) replaces the exit slit body. Each of the 2500 pixel columns on the CCD chip is 12 microns wide, providing a total spectral coverage of 24 nm and a step size of 0.0096 nm.

I_2 vapor, at pressures ranging from 20 to 160 milliTorr, was held in a glass and fused silica cell, equipped with Brewster angle laser inlet and exit windows. The cell was filled on a glass vacuum line pumped by a diffusion pump/mechanical pump combination to a base pressure of $\approx 2 \times 10^{-5}$ Torr. All pressures were measured with a capacitance manometer (MKS Baratron 127 series) with a precision of ± 1 milliTorr. I_2 (Aldrich, 99.999%) was used without additional purification.

$E-D$ Franck–Condon factors have been calculated using the LEVEL program from Rydberg–Klein–Rees (RKR) potential energy curves for the E and D electronic states.[26] The E state curve used was determined using the spectroscopic data of Brand *et al.*[27] We utilized directly the RKR curve for the D state provided by Ishiwata and Tanaka.[28]

III. RESULTS

In Fig. 2, we display the ultraviolet portion of the emission spectrum that results when low pressure (40 milliTorr) I_2 is excited to the E electronic state, $v=0$, $J=55$. The discrete peaks clustered about 335 nm are the well-assigned E
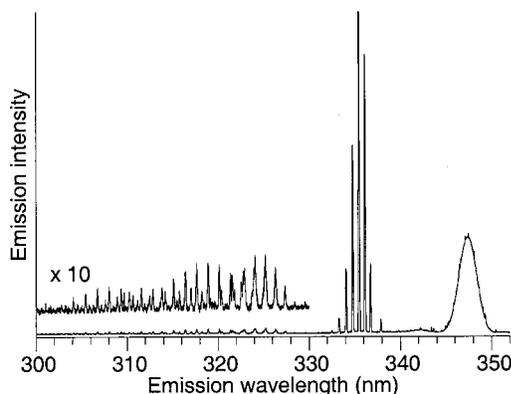
FIG. 2. Ultraviolet portion of the emission spectrum that result from excitation of I_2 in the E ion-pair state, $v=0$, $J=55$. The I_2 pressure is 40 milliTorr.

$\rightarrow A$ ($\Omega=1_u$) emission transitions.[22] These perpendicular transitions ($\Delta\Omega=+1$) are approximately 2 orders of magnitude less intense than the ≈ 425 nm, $E\rightarrow B$ transitions (not shown) which dominate emission from the E state. The continuous feature centered at 347 nm is the $E\rightarrow B''$ bound-free spectrum.[22] The B'' state is a repulsive, $\Omega=1_u$ electronic state which correlates with two $^2P_{3/2}$ I atoms.

In this paper, we focus on the weak emission observed between 300 and 330 nm, assigned to $D\rightarrow X$ vibronic transitions. In Fig. 3 we show this region on an expanded scale, along with our fit to this spectrum. In our spectral simulations, the populations of the $v=0-6$ vibrational levels in the D state are variable parameters. (Higher energy vibrational levels in the D state are found to lack statistically significant population.) With spectral resolution of ≈ 0.2 nm, we are unable to resolve $D\rightarrow X$ rotational structure, but we do find that the quality of the fit is sensitive to the breadth of the rotational distribution that we assume is populated in the D
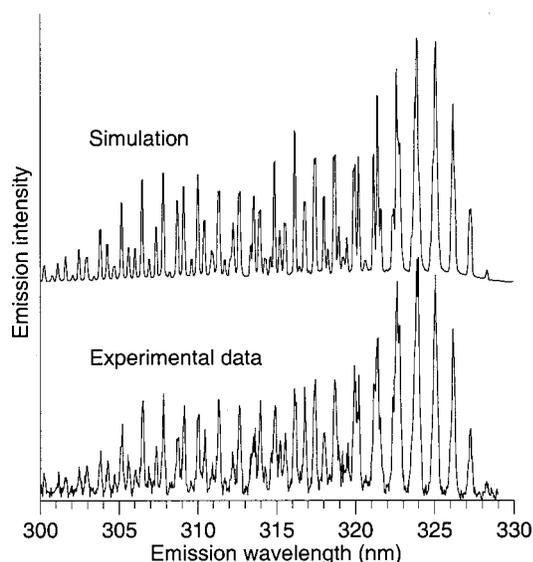
state. Following a model used frequently for collision-induced rotational relaxation,[29] we treat the rotational population of the D state using a power law,

$$P(J_f) \propto (2J_f+1)\left(\frac{\Delta E_{\mathrm{rot}}}{B_v}\right)^{-\alpha},$$

where $P(J_f)$ is the probability of observing rotational level J_f, B_v is the rotational constant for the vibrational level in question, and ΔE_{rot} is the difference in energy between the level J_f and the level J_i that is populated in the D state if no rotational relaxation/excitation accompanies the electronic energy transfer. (For $E\rightarrow D$ electronic energy transfer, a change in electronic inversion symmetry occurs. When we populate $J=55$ in the E state, for example, preservation of nuclear spin symmetry dictates that only the even J rotational levels are populated in collision-induced transfer to the D state. We assume that the most populated rotational level in the D state is $J=54$. When $J=98$ is populated in the E state, we assume that $J=97$ is the most populated level in the D state.)

In our fits to the $D\rightarrow X$ spectra that result when either $J=55$ or 98 is initially prepared in the E state, we find that $\alpha\approx 0.7$ provides the best overall agreement with the experimental data. (We find that the vibrational population distributions discussed below are relatively insensitive to the value of α, however.) Because of our limited spectral resolution, we have made no attempt to fine tune the α parameter to take into account the likely event that different distributions of rotational levels are populated in different vibrational levels in the D state. Similarly, we cannot confirm that the power law model assumed is more or less valid for these collision events than any other model of the distribution of rotational population. We find it a useful approach to demonstrate two critical aspects of our results. First, the breadth of the $D\rightarrow X$ spectral features observed dictate that a distribution of D state rotational levels are populated in the collisions. Second, the distribution of rotational population is centered about the rotational level corresponding to no change in I_2 rotational angular momentum.

In Fig. 4 and Table I, we display the vibrational level population distributions that we derive from the spectral

FIG. 3. $D\rightarrow X$ emission spectrum resulting from the excitation of an 40 milliTorr sample of I_2 to the E ion-pair state, $v=0$, $J=55$. The lower panel shows the experimental data, while the upper panel is a simulation incorporating the best fit D state vibrational populations.
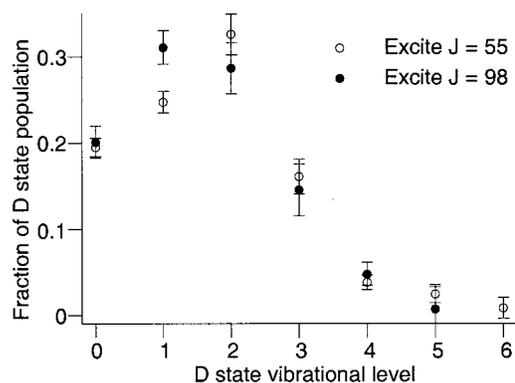

FIG. 4. D electronic state vibrational populations following excitation of two different rotational levels in the ground vibrational state of the E state. The open circles refer to $J=55$ excitation; the closed circles to $J=98$ excitation.

TABLE I. $E \rightarrow D$ vibrational branching fractions and Franck–Condon factors.

	Fraction of D state population		$|\langle E_{v=0}|D_v\rangle|^2$	
D state v	$J=55$	$J=98$	$J=55$	$J=98$
0	0.195	0.201	0.663	0.669
1	0.248	0.311	0.294	0.290
2	0.326	0.287	4.09×10^{-2}	3.92×10^{-2}
3	0.161	0.146	1.94×10^{-3}	1.79×10^{-3}
4	0.038	0.048	2.00×10^{-5}	1.72×10^{-5}
5	0.024	0.007	1.82×10^{-10}	1.39×10^{-9}
6	0.008		3.69×10^{-9}	4.57×10^{-9}

simulations. Qualitatively, the D state distributions that result from excitation of $J=55$ and 98 in the E state are quite similar, with $v=0-3$ accounting for more than 92% of the total. Indeed, with the exception of a somewhat higher population in $v=1$ when $J=98$ is initially excited in the E state, the distributions are identical, within experimental error.

We have carried out a study to determine the dependence of the $D \rightarrow X$ emission intensity on I$_2$ pressure to assure that the signals observed are truly collision induced. In Fig. 5, we present the results of this study, demonstrating that the ratio of the $D \rightarrow X$ integrated signal to the integrated $E \rightarrow A$ signal grows linearly with I$_2$ pressure. Since the $E \rightarrow A$ signal itself increases linearly with I$_2$ pressure, the $D \rightarrow X$ signals increase with the square of I$_2$ pressure, as expected for a bimolecular collision-induced process.

The data presented in Fig. 5 is for E state, $J=98$ excitation, and the $D \rightarrow X$ signals are well behaved throughout the pressure range examined. When we prepare $J=55$ in the E state, however, we observe anomalous $D \rightarrow X$ emission signals at intermediate (80 milliTorr) I$_2$ pressures and higher. In Fig. 6, we show emission spectra that result from excitation of $J=55$ in the E state for two different I$_2$ pressures. When the sample is 40 milliTorr of I$_2$ a spectrum (Fig. 6, lower panel) like that described previously is observed. The vibrational populations (Fig. 4) obtained from this spectrum are independent of the I$_2$ pressure, as long as the pressure is low (i.e., 20–40 milliTorr). In the upper panel, we observe that the $D \rightarrow X$ emission signal is dramatically more intense when
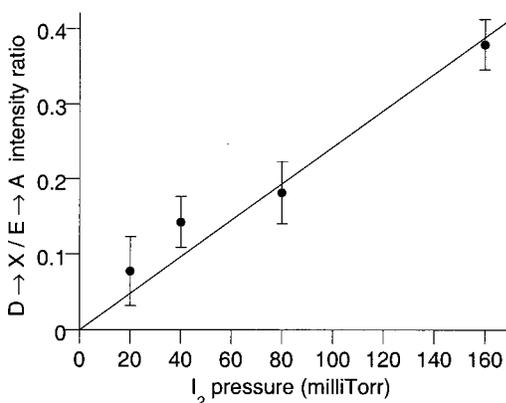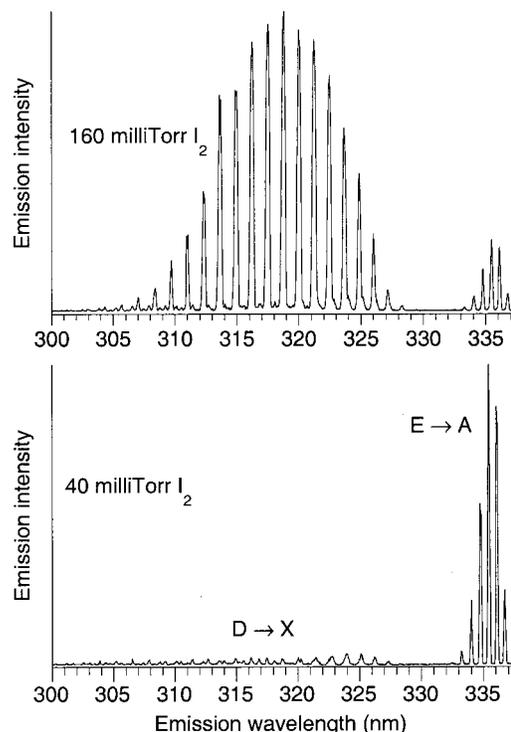

FIG. 6. Anomalous pressure dependence of the D state emission features resulting from excitation of $J=55$ in the ground vibrational state of the E state. In the lower panel, the I$_2$ pressure is 40 milliTorr; in the upper panel the I$_2$ pressure is 160 milliTorr.

the I$_2$ pressure is 160 milliTorr. (The $D \rightarrow X/E \rightarrow A$ integrated intensity ratio has grown 75-fold with a 4-fold increase in pressure.) The $D \rightarrow X$ Franck–Condon profile indicates that primarily $v=0$ in the D state is populated, in contrast to the broader vibrational distribution displayed in Fig. 4. Vestiges of the more diffuse $D \rightarrow X$ emission pattern characteristic of lower pressures are observed in the baseline.

The anomalous $D \rightarrow X$ signals also differ from the data considered here in their dependence on the delay between the two excitation laser pulses. The intensity of the collision-induced signal displayed in Fig. 6 (lower) decays slowly with increasing delay between the laser pulses, over a range of several hundred nanoseconds. This behavior is consistent with the long lifetime of the B electronic state ($\tau_0 = 0.890 \, \mu$s for $v=20$),[13] and is further evidence that the $D \rightarrow X$ signals arise from collisions that occur following excitation to the E state. The anomalous emission, on the other hand, is more strongly dependent on the delay between laser pulses. These signals are smaller by a factor of 10 if the lasers are not overlapped temporally, and then decay further with increasing delay between the lasers. The anomalous emission is indistinguishable from the more diffuse $D \rightarrow X$ signals when the delay reaches ≈ 150 nanoseconds. Clearly, an entirely different process is responsible for this new emission pattern, though we cannot discern a single mechanism that is consistent with all of the experimental data. The sharp dependence of the anomalous features on the temporal overlap of the laser pulses suggests a collision-induced process involving a repulsive intermediate state. We note that the lower energy laser photon in our excitation scheme is ca-

FIG. 5. I$_2$ pressure dependence of the ratio of the $D \rightarrow X$ to $E \rightarrow A$ emission signals. The line represents the best linear fit that also includes the origin.
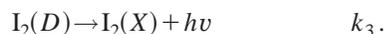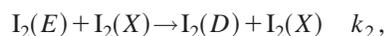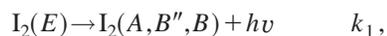
pable of accessing the repulsive wall of one or more I_2 electronic states correlating with ground state I atoms from the inner turning point of the X state potential. Approximately 1% of such excited species can undergo a collision during the 10 nanosecond pulse width of our lasers (assuming a 60 $Å^2$ cross section, typical of the collision-induced quenching of the B state).[13] If such a collision results in g/u mixing then either the higher energy laser photons or a portion of the intense $E \rightarrow B$ emission can provide direct excitation to the D state. This excitation scheme requires, however, temporal overlap of the lasers as the proposed intermediate state is short lived. When the lasers are not overlapped in time, we suggest that collisions mixing the B and either the $a(1_g)$ or $a'(0_g^+)$ states occur, resulting in direct excitation of the D state by either absorption of the higher energy laser photons or reabsorption of a portion of the $E \rightarrow B$ emission photons. These phenomena occur in our $J=55$ excitation scheme (but not $J=98$) presumably because of an unfortunate convergence of resonant frequencies. To avoid the impact of these anomalous signals, we have focused our analysis on low I_2 pressures ($\leqslant 40$ milliTorr) when $J=55$ is initially excited, and on excitation of $J=98$. In the latter case the data are free of the anomalous signals for the entire range of pressures examined (i.e., up to 160 milliTorr).

The insensitivity of the D state vibrational distributions to I_2 pressure, and the linear I_2 pressure dependence of D state emission intensity (relative to the E state emission intensity) allow us to assume that single collision conditions exist for these low pressure samples. Under these conditions, the following three processes occur following excitation of I_2 to the E state:

$$I_2(E) \rightarrow I_2(A,B'',B) + h\upsilon \qquad k_1,$$
$$I_2(E) + I_2(X) \rightarrow I_2(D) + I_2(X) \quad k_2,$$
$$I_2(D) \rightarrow I_2(X) + h\upsilon \qquad k_3.$$

Using standard kinetic analysis, the rate equations describing these processes may be integrated to yield the following expression for the ratio of emission intensities from the E and D electronic states:

$$\frac{I_D}{I_E} = \frac{k_2[I_2(X)]}{k_1}.$$

Lawley et al. have determined the emission lifetimes and Einstein A coefficients for the ion-pair to valence electronic transitions.[30] Using these data, we can convert our measurements of $D \rightarrow X / E \rightarrow A$ emission intensity ratios to I_D/I_E, and then determine k_2, the bimolecular rate constant for electronic energy transfer. The resulting value for k_2, averaged over all pressures, is $4.0 \pm 0.7 \times 10^{-17}$ $m^3 s^{-1}$ molecule^{-1}. Since in hard sphere collision theory $k = \sigma \upsilon$, we can use the mean relative velocity of I_2 molecules at room temperature, $\upsilon = 223$ m/s, to determine that the effective hard sphere cross section for electronic energy transfer is 18 ± 3 $Å^2$.

Yamasaki and Leone derived the following expression for calculating the probability, P_n, that a molecule undergoes n collisions in time Δt:
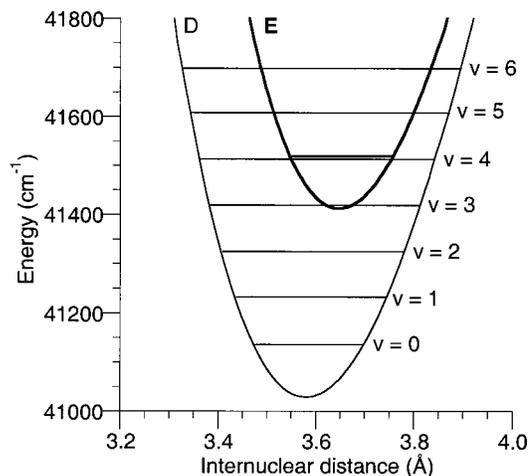

FIG. 7. E electronic state (heavy line) and D electronic state (light line) potential energy curves. The energies of the vibrational states ($J=55$) are superimposed on the plots.

$$P_n = \frac{1}{n!}\left(\frac{\upsilon \Delta t}{\lambda}\right)^n e^{-\upsilon \Delta t/\lambda},$$

where υ is the mean relative velocity and λ is the mean free path.[31] Using an effective cross section of 18 $Å^2$ and an I_2 pressure of 160 milliTorr, we find that the probability of an I_2 molecule having zero collisions, P_0, in 125 nanoseconds [≈ 5 times the lifetime of $I_2(E)$] is 0.974. P_1, the probability of one collision, is 0.0253. The probability of having more than one collision $(1 - P_0 - P_1)$ is 6.7×10^{-4}. Thus, fewer than 3% of the molecules involved in collisions suffer more than one encounter, validating our assumption of single collision conditions over the entire pressure range considered.

IV. DISCUSSION

In Fig. 7 we display portions of the E and D electronic potential energy curves, illustrating specifically the relative energies of the vibrational levels populated in this study. This figure clearly demonstrates that the D state vibrational levels that are populated by electronic energy transfer are not those that are nearly in resonance with the initially excited E state level. For $J=55$, the energy gap between $v=0$ in the E state and $v=4$ in the D state is less than 9 cm^{-1}. The data demonstrates, however, that less than 4% of all D state molecules are found in $v=4$. The predominantly populated D state levels, $v=0, 1, 2,$ and 3, have energy gaps ($J=55$) of 386, 291, 197, and 102 cm^{-1}, respectively. Clearly, the electronic energy transfer process that originates in $v=0$ of the E state does not favor population of vibrational states with small energy gaps.

An alternative approach to understanding the pattern of vibrational level populations is to consider the vibrational overlap integrals that link the E and D electronic states. The applicability of the Franck–Condon model to electronic energy transfer processes has been controversial and not consistently reliable.[23,32] In Table I, we tabulate the relevant $E-D$ Franck–Condon factors, along with the observed vibrational branching fractions. Qualitatively, the experimental data suggests that the vibrational populations are determined

J. Chem. Phys., Vol. 115, No. 9, 1 September 2001

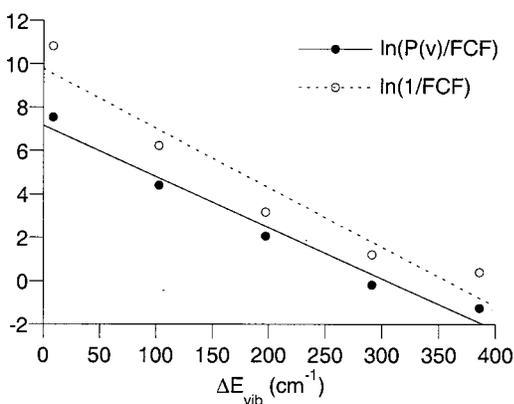Electronic energy transfer in I₂   4137

FIG. 8. Plots showing generally good agreement of the experimental data with a model that incorporates both Franck–Condon and energy gap effects (see text for details).

by the degree of Franck–Condon overlap between the initial and final vibrational states. The lowest vibrational states in the D state have the greatest Franck–Condon overlap with E, $v=0$, and are the most highly populated. Thus, while considerations based on energy gaps alone are clearly erroneous, the Franck–Condon model does reproduce certain gross features of the data. Noting that the vibrational populations do not decrease with v as fast as the Franck–Condon factors would suggest, it is tempting to combine the energy gap and Franck–Condon effects, and to write the probability, $P(v)$, of populating vibrational level v in the hybrid form:

$$P(v) = K(\text{FCF})e^{-\Delta E_{\text{vib}}/\beta},$$

where K is a proportionality constant, ΔE_{vib} is the vibrational energy gap, and β is a variable parameter. Such a form was proposed by Katayama $et\ al.$ and was found to reproduce the vibrational branching that occurs in collision-induced electronic energy transfer in N_2^+.[33] In Fig. 8 we plot the $J=55$ vibrational branching fractions for the exoergic channels (populating D state, $v=0$–4) using the rearranged form

$$\ln\left(\frac{P(v)}{\text{FCF}}\right) = \ln K - \frac{\Delta E_{\text{vib}}}{\beta}.$$

The near linearity of the plot (filled circles in the figure) is suggestive of excellent agreement between the model and the experimental data. Also shown in Fig. 8, however, is the plot of $\ln(1/\text{FCF})$ verses ΔE_{vib} (open circles), revealing that the dominant determinant of the agreement with the model is the variation of the Franck–Condon factors with ΔE_{vib}. Since this functional dependence is purely coincidental, we cannot draw any quantitative conclusions about the adequacy of the hybrid model. It is reasonable to assert, however, that a propensity for small vibrational energy gaps appears to play a role in moderating the impact of the Franck–Condon factors, though we cannot determine whether the model incorporates this effect correctly.

One explanation, therefore, for the observation that the vibrational distributions peak at $v>0$ is this balance between Franck–Condon overlap and vibrational energy gap. An alternative is to note that the energy gaps associated with

population of $v=1$ and 2 in the D state are 291 and 197 cm^{-1}, respectively for $J=55$, 287, and 193 cm^{-1}, respectively for $J=98$. These values are not too different from the spacing between $v=0$ and $v=1$ in ground state I_2, 213.3 cm^{-1}.[34] These energy gaps may be particularly favored because the $I_2(X)$ collision partner can be vibrationally excited in a collision-induced transfer of vibrational energy that minimizes the magnitude of the involvement of the translational or rotational degrees of freedom.

The distribution of D electronic state vibrational energy that we report here is similar to those reported in earlier investigations. Inard $et\ al.$, in their study of the relaxation of $v=1$ in the E state, find that the D state level that is most populated is separated from the initial state by an energy that is approximately the same as the vibrational frequency in $I_2(X)$.[22] Teule $et\ al.$, examined the D state emission that occurs following excitation of $v=8$, 9, 13, and 15 in the E state.[21] The vibrational distributions observed in these experiments defy simple explanation, as the predominant pathway for some of the initial states is near resonant transfer, while in at least one case (excitation of $v=8$), Franck–Condon effects appear to outweigh the impact of substantial energy gaps.[21] Perhaps significantly, Franck–Condon effects appear to be most important when the mismatch in energy between the initially excited E state level and the closest D state level is relatively large ($\geqslant 25$ cm^{-1}). When a pathway with a small energy mismatch ($\leqslant 10$ cm^{-1}) is available, then the near resonant transfer occurs, in spite of small Franck–Condon overlap. We note, however, that the relevant $E-D$ Franck–Condon factors for these higher E state vibrational levels exhibit a variation of at most a factor of 100, while we report in Table I a range of 10^8 for $v=0$. Perhaps pathways with small energy gaps can be favored, despite less favorable vibrational overlaps, but only if the Franck–Condon discrepancy is not too great. Teule $et\ al.$ also suggest that an enhancement of the cross section may occur whenever there is an opportunity to vibrationally excite the $I_2(X)$ collision partner, which our data tend to support.[21] The upper limit for the cross section for $E \rightarrow D$ electronic energy transfer derived by Teule $et\ al.$, 30 Å^2,[21] is fully consistent with the 18 Å^2 value that we have deduced.

All of these investigations stand in contrast, however, to the work of Akopyan $et\ al.$, in which $E \rightarrow D$ collision-induced energy transfer is found to be much more efficient and selective, in terms of the range of D state vibrational levels populated.[24,25] In this work, the cross section for electronic energy transfer is large, $>10^3$ Å^2, and dominated by near resonant energy transfer. Several E state vibrational levels were investigated, and in each case the D state level closest in energy was most populated, without regard to the degree of Franck–Condon overlap between the vibrational wave functions. Significant population of D state levels with larger energy gaps was also observed, but with probabilities that are approximately an order of magnitude lower than the near resonant pathways.[24,25]

It is difficult to reconcile the inconsistencies in the experimental results described at this time. The work of Akopyan $et\ al.$ treats E state vibrational levels that are somewhat higher ($v=23$–55) than any of the other investigations, and

a facile explanation is that an entirely different mechanism for electronic energy transfer is operable for high vibrational levels in the E state. For the lower vibrational levels, however, a consistent model appears to emerge from the accumulated experimental data. As long as the energy gaps are not too small, Franck–Condon effects appear to play a role in determining the distribution of vibrational energy in the D state. This trend is modulated, however, by a significant propensity to populate those vibrational levels whose energy gaps come close to providing the right amount of energy to vibrationally excite the $I_2(X)$ collision partner. When very near-resonant $E \rightarrow D$ energy transfer pathways ($\Delta E_{vib} \leq 10 \, cm^{-1}$) are available, however, those pathways are preferred as long as there is not too large a disincentive provided by very poor vibrational wave function overlap.

McKendrick has reviewed the vibrational energy distributions that result from electronically inelastic collisions of SiCl and SiF with rare gas atoms.[35] Despite their chemical similarity, these species exhibit strikingly different behavior. The vibrational populations in SiF are correlated with Franck–Condon factors. In SiCl, however, the vibrational distributions do not exhibit any particular pattern. McKendrick suggests a plausible model that invokes a curve crossing in the isolated SiCl molecule, with the implication that multiple recrossings of this seam in the intermolecular potential destroys the ''sudden'' nature of the vibrational distributions.[35] It is difficult to imagine that such a model can explain the vibrational energy dependence of the D state distributions in the case of $I_2(E) + I_2(X)$ collisions. The isolated molecule potential energy curves are relatively free of perturbations, particularly those that might mix g and u states. The highest vibrational level explored, $v = 55$ in the E state, lies at an energy that is less than 20% of the total E state well depth. The RKR potential energy curves show that, at this energy, the D and E I_2 curves remain separate, with the E curve nested within that of the D electronic state. Thus, we find no evidence for an isolated molecule perturbation that might induce a dramatic change in the mechanism for electronic energy transfer. Clearly, additional experimental and theoretical attention to the rich and diverse collision-induced behavior of the diatomic halogens in their ion-pair electronic states is warranted.

Note added in proof. In a forthcoming paper,[36] we demonstrate that the D electronic state vibrational distributions that result from collisions of $I_2(E)$ with either He or Ar are qualitatively similar to that observed from $I_2(E) + I_2(X)$ collisions. Thus, the role of vibrational excitation of the collision partner may be less important than suggested in the preceding discussion.

ACKNOWLEDGMENTS

[1] R. W. Wood, Philos. Mag. **21**, 309 (1911); J. Franck and R. W. Wood, *ibid.* **21**, 314 (1911).

[2] J. I. Steinfeld and W. Klemperer, J. Chem. Phys. **42**, 3475 (1965).

[3] R. B. Kurzel and J. I. Steinfeld, J. Chem. Phys. **53**, 3293 (1970).

[4] J. I. Steinfeld and A. N. Schweid, J. Chem. Phys. **53**, 3304 (1970).

[5] R. B. Kurzel, J. I. Steinfeld, D. A. Hatzenbuhler, and G. E. Leroi, J. Chem. Phys. **55**, 4822 (1971).

[6] D. J. Krajnovich, K. W. Butz, H. Du, and C. S. Parmenter, J. Chem. Phys. **91**, 7705 (1989).

[7] D. J. Krajnovich, K. W. Butz, H. Du, and C. S. Parmenter, J. Chem. Phys. **91**, 7725 (1989).

[8] H. Du, D. J. Krajnovich, and C. S. Parmenter, J. Phys. Chem. **95**, 2104 (1991).

[9] S. L. Dexheimer, M. Durand, T. A. Brunner, and D. E. Pritchard, J. Chem. Phys. **76**, 4996 (1982).

[10] S. L. Dexheimer, T. A. Brunner, and D. E. Pritchard, J. Chem. Phys. **79**, 5206 (1983).

[11] W. G. Lawrence, T. A. Marter, M. L. Nowlin, and M. C. Heaven, J. Chem. Phys. **106**, 127 (1997).

[12] J. E. Selwyn and J. I. Steinfeld, Chem. Phys. Lett. **4**, 217 (1969).

[13] G. A. Capelle and H. P. Broida, J. Chem. Phys. **58**, 4212 (1973).

[14] J. Derouard and N. Sadeghi, Chem. Phys. Lett. **102**, 324 (1983).

[15] U. K. A. Klein, J. Mastromarino, and A. Suwaiyan, Chem. Phys. Lett. **217**, 86 (1994).

[16] K. Nakagawa, M. Kitamura, K. Suzuki, T. Kondow, T. Munakata, and T. Kasuya, Chem. Phys. Lett. **106**, 259 (1986).

[17] X. Zheng, S. Fei, M. C. Heaven, and J. Tellinghuisen, J. Chem. Phys. **96**, 4877 (1992).

[18] T. Ishiwata, S. Motohiro, E. Kagi, H. Fujiwara, and M. Fukushima, Bull. Chem. Soc. Jpn. **73**, 2255 (2000).

[19] W. Ubachs, I. Aben, J. B. Milan, G. J. Somsen, A. G. Stuiver, and W. Hogervorst, Chem. Phys. **174**, 285 (1993).

[20] U. Heemann, H. Knöckel, and E. Tiemann, Chem. Phys. Lett. **90**, 17 (1982).

[21] R. Teule, S. Stolte, and W. Ubachs, Laser Chem. **18**, 111 (1999).

[22] D. Inard, D. Cerny, M. Nota, R. Bacis, S. Churassy, and V. Skorokhodov, Chem. Phys. **243**, 305 (1999).

[23] P. J. Dagdigian, Annu. Rev. Phys. Chem. **48**, 95 (1997).

[24] M. E. Akopyan, N. K. Bibinov, D. B. Kokh, A. M. Pravilov, M. B. Stepanov, and O. S. Vasyutinskii, Chem. Phys. **242**, 263 (1999).

[25] M. E. Akopyan, N. K. Bibinov, D. B. Kokh, A. M. Pravilov, O. L. Sharova, and M. B. Stepanov, Chem. Phys. **263**, 459 (2001).

[26] University of Waterloo Chemical Physics Research Report No. CP-230R3, 1986.

[27] J. C. D. Brand, A. R. Hoy, A. K. Kalkar, and A. B. Yamashita, J. Mol. Spectrosc. **95**, 350 (1982).

[28] T. Ishiwata and I. Tanaka, Laser Chem. **7**, 79 (1987).

[29] T. A. Brunner and D. Pritchard, Adv. Chem. Phys. **50**, 589 (1982).

[30] K. Lawley, P. Jewsbury, T. Ridley, P. Langridge-Smith, and R. Donovan, Mol. Phys. **75**, 811 (1992).

[31] K. Yamasaki and S. R. Leone, J. Chem. Phys. **90**, 964 (1989).

[32] M. H. Alexander and G. C. Corey, J. Chem. Phys. **84**, 100 (1986).

[33] D. H. Katayama, T. A. Miller, and V. E. Bondybey, J. Chem. Phys. **71**, 1662 (1979).

[34] F. Martin, R. Bacis, S. Churassy, and J. Vergès, J. Mol. Spectrosc. **116**, 71 (1986).

[35] K. G. McKendrick, J. Chem. Soc., Faraday Trans. **94**, 1921 (1998).

[36] C. J. Fecko, M. A. Freedman, and T. A. Stephenson, J. Chem. Phys. (to be submitted).